NUCL SCI TECH (2017) 28:20
DOI 10.1007/s41365-016-0171-x

Measurement and Monte Carlo simulation of γ-ray dose rate in high-exposure building materials

A. Abbasi[1,2] · M. Hassanzadeh[1]

Received: 3 May 2016 / Revised: 28 August 2016 / Accepted: 29 August 2016 / Published online: 26 December 2016

Abstract Natural radioactivity radionuclides in building materials, such as ^{226}Ra, ^{232}Th and ^{40}K, cause indoor exposure due to their gamma-rays. In this research, in a standard dwelling room (5.0 m × 4.0 m × 2.8 m), with the floor covered by various granite stones, was set up to simulate the dose rates from the radionuclides using MCNP4C code. Using samples of granite building products in Iran, activities of the ^{226}Ra, ^{232}Th and ^{40}K were measured at 3.8–94.2, 6.5–172.2 and 556.9–1529.2 Bq kg^{-1}, respectively. The simulated dose rates were 26.31–184.36 nGy h^{-1}, while the measured dose rates were 27.70–204.17 nGy h^{-1}. With the results in good agreement, the simulation is suitable for any kind of dwelling places.

Keywords Radioactivity · Building materials · Absorbed dose · Experimental · MCNP4C

1 Introduction

Indoor exposure to gamma-rays from natural radionuclides in building materials is inherently greater than outdoor exposure [1]. To determine radiological hazards to human health, the natural radioactivity from building materials must be under control. Some researchers measured radioactivity in concrete, granites and sand [2]. Terrestrial origin building materials, such as concrete, cement, brick, sand, aggregate, marble, gypsum and granite [3], usually contain the uranium and thorium decay series radionuclides, so the radiation exposure arises mainly from ^{238}U, ^{232}Th series and ^{40}K [4]. When the duration of occupancy is taken into account, indoor exposure becomes even more significant [5].

The distribution and concentrations of the parent radium radionuclides in bedrocks of various types vary greatly from type to type. In general, granites have relatively high radium content. Therefore, it is not only important but also feasible to assess the radiological hazard by calculating indoor external dose based on radioactivity measured for building materials [6]. Radium-226, as an alpha emitter with a half-life of 1622 years, is a natural decay product of ^{238}U series. The other gamma-emitting radionuclides from ^{226}Ra decay are ^{214}Pb and ^{214}Bi.

The specific absorbed dose rate in air is mainly affected by the following parameters: position, thickness and density of building materials [7, 8]. The Monte Carlo code MCNP4C has been used to evaluate the absorbed doses in air. Developed for simulating transports of electrons, neutrons, photons, etc., the code gives an arbitrary three-dimensional configuration of materials in geometric cells. The model has been presented in terms of an input file in this code. It encloses the geometry, material, source information and the type of output needed in the form of standard tallies already supplied [9].

In this paper, in a living room geometry, dose rates of ^{226}Ra, ^{232}Th and ^{40}K in high-exposure building materials in Iran are measured and simulated using the MCNP4C code. The simulation and measurement results are compared.

✉ M. Hassanzadeh
m_hassanzadeh1354@yahoo.com;
mhasanzadeh1354@gmail.com

1 Reactor Research School, Nuclear Science and Technology Institute (NSTRI), P.O. Box 141551339, Tehran, Iran

2 University of Kyrenia, Kyrenia, North Cyprus, Mersin 10, Turkey

2 Materials and methods

2.1 Experimental procedure

The collected samples were pulverized, sieved through a 0.2-mm mesh, sealed in standard 1-L Marinelli beakers, dry-weighed and stored for 4 weeks before counting in order to allow the attainment of equilibrium between ^{226}Ra and ^{222}Rn and its decay products. In equilibrium, the activity of each daughter is equal to that of the initial isotope of the series [8]. The gamma-ray spectra of the prepared samples were measured using a typical high-resolution gamma spectrometer based on a coaxial P-type shielded high-purity germanium (HPGe) detector, with a relative photo-peak efficiency of 80% and energy resolution of 1.80 keV (FWHM) at 1332 keV, coupled to a high-count-rate Multi-Task 16 k MCA card. Commercial software Gamma Genie-2000 was used for data analysis [6].

The ^{226}Ra activities were calculated from the short-lived daughters ^{214}Pb (295.2 and 351.9 keV) and ^{214}Bi (609.3 keV). Similarly, ^{232}Th activities were measured by taking the mean activity of photo-peaks of the daughter nuclides ^{228}Ac (338.40, 911.07 and 968.90 keV) and ^{212}Pb (238.63 keV). Activities of ^{40}K were determined directly from its 1460.83 keV gamma-ray. Quality assurance of the measurements was determined by using of Standard Reference Material IAEA Soil-375 [10].

The density of all the granite samples was estimated at 2580 kg m^{-3} in average. The granite stones in markets are usually sized at 30 cm × 50 cm × 3 cm [11]. The granites differ from one type to another in their compositions. Table 1 shows the composition of a typical granite stone.

Calculation of the dose rate conversion factors was done based on the point kernel integration method for floors covered with 3.0-cm-thick granite. The free-in-air absorbed dose rate (nGy h^{-1}) in the room center can be expressed as Eq. (1) [4]:

$$\mathrm{d}D/\mathrm{d}t = 0.04A_{\mathrm{K}} + 0.46A_{\mathrm{Ra}} + 0.60A_{\mathrm{Th}}, \tag{1}$$

where A_{K}, A_{Ra} and A_{Th} are the activity concentrations (Bq kg^{-1}) of ^{40}K, ^{226}Ra and ^{232}Th, respectively.To calculate the effective annual dose rate (mSv), we consider the conversion factor 0.7 Sv Gy^{-1} for adult categories. The indoor occupancy factor is 0.8 as given by UNSCEAR report, and the allowed indoor dose is 1 mSv year^{-1} [5]. The effective annual dose rate is given by Eq. (2)

Table 1 Compositions (in %) of a typical granite sample

Fe_2O_3	FeO	CaO	Na_2O	K_2O	Al_2O_3	SiO_2
1.22	1.68	1.82	3.69	4.12	14.42	72.04

$$\mathrm{d}E/\mathrm{d}t = (\mathrm{d}D/\mathrm{d}t) \times 0.7\,(\mathrm{Sv\,Gy^{-1}}) \times 24 \times 365 \times 0.8\,(\mathrm{h\,year^{-1}}). \tag{2}$$

2.2 Theoretical procedure

2.2.1 Room geometry

According to the standard living room, a room with dimensions of 4.0 m × 5.0 m × 2.8 m is defined for the MC simulation. Its floor is covered with granite stones of 3.0 cm thickness, with the compositions listed in Table 1. The detector is at the room center.

2.2.2 Monte Carlo simulation

By defining necessary parameters of high-exposure building materials and room geometry, we can simulate the indoor external gamma-ray exposure and the dose distribution. The interaction of photons with walls and the air is simulated by MCNP4C code.

To improve the calculation accuracy, 10–2000 keV gamma-rays of over 1% emission intensity from ^{226}Ra, ^{232}Th and ^{40}K, as summarized in Table 2, are used in the simulation.

The photon flux and energy deposition in the room center are calculated by using *F*4 and *F*6 tallies, respectively. This code reads the input file such as the geometry, materials, neutron source. Results of interest can be scored by using tallies. A tally is a specification of what should be included in the output. For example, the photons flux (*F*4) through a certain area or the number of photons in a particular energy interval can be calculated by [9]

$$F4 = C\int \Phi(E)\mathrm{d}E, \tag{3}$$

where C is an arbitrary scalar quantity for normalization, $\Phi(E)$ is the photon flux (*F*4) in cm^{-2}, and E is incident photon energy.The energy deposition or heating tally (*F*6) is the following track length estimates and can be calculated by

$$F6 = \rho_{\mathrm{a}}/\rho_{\mathrm{g}}\int H(E)\Phi(E)\mathrm{d}E, \tag{4}$$

where ρ_{a} is the atom density (atoms barn^{-1} cm^{-1}); ρ_{g} is the mass density (g cm^{-3}); and $H(E)$ is the heating response, having different meanings, depending upon the context as follows

$$H(E) = \sigma_{\mathrm{T}}(E)H_{\mathrm{avg}}(E), \tag{5}$$

Table 2 Gamma energies emission from ^{226}Ra, ^{232}Th series and ^{40}K with intensity higher than 1%

^{232}Th	E (keV)	39	57.7	63.7	84.4	99.5	129	154	209	238	241	277	338	510	583	727	860	911	969	2614
	Intensity (%)	1.9	4.8	3.8	1.2	1.2	2.4	6.2	3.9	2.9	4.1	6.8	11.4	21.6	84.2	11.8	12.5	27.7	16.6	100
^{226}Ra	E (keV)	46	63	92	295	352	609	1120	1238	1764	2204						^{40}K E (keV)			1461
	Intensity (%)	3.9	3.8	5.4	19.2	37.2	46.3	15.1	5.9	15.8	5.0						Intensity (%)			10.7

where σ_T is total photon cross section and $H_{avg}(E)$ is average energy of exiting gamma-rays for each reaction and for all energies is assumed to be deposited locally. The energy deposition tally ($F6$) is in MeV g^{-1}.

3 Results and discussion

3.1 Experimental and simulation results

The measured activities of ^{232}Th, ^{226}Ra and ^{40}K in the granite samples are 6.5–172.2, 3.8–94.2 and 556.9–1529.2 Bq kg^{-1}, respectively. They are shown in Table 3, together with measurement and simulation results of the absorbed dose rate (dD/dt) and effective annual dose rate (dE/dt) due to ^{226}Ra, ^{232}Th and ^{40}K in air.

The absorbed dose rate is calculated by using *DFn* (Dose Function), *DEn* (Dose Energy) cards and tally *F*4 operations. Suppose one wanted to compute a dose rate of some type associated with a flux tally, either total or by energy group. This feature allows one to enter a point-wise response function (such as flux-to-dose conversion factors) as a function of energy to modify a regular tally. The energy points are specified on the *DEn* card, and the corresponding values of the dose function are identified on the *DFn* card.

The calculated dose rate distributions due to ^{232}Th, ^{226}Ra and ^{40}K in the room floor are shown in Fig. 1. As can be seen, the dose rate in the floor center is the maximum. The dose rate decreases with increasing height (the **Z** direction, not shown).

The simulated dose rates are 26.3–184.4 nGy h^{-1}, averaged at 90.7 nGy h^{-1}, while the measured dose rates are 27.7–204.2 nGy h^{-1}, averaged at 104.9 nGy h^{-1}. The two sets of minimum–maximum range and average value overlap closely. Thus, the simulation method is suitable to any kind of dwelling places with the use of granite stones. The uncertainties are calculated within 1σ (standard deviation) and simulation uncertainties calculated fewer than 5% errors by code. The uncertainty is calculated by

$$X_{mean} = \left(\sum X_i\right)/N, \quad \sigma_X = \left[\sum (X_i - X_{mean})^2/N\right]^{1/2},$$
$$X = X_{mean} \pm \sigma_X, \tag{6}$$

where X_{mean} is the mean value, N is number of data, and X_i is data ($i = 1,2,3,\ldots,N$). The approximations errors are expressed by:

$$\mathrm{Rel}(X_A) = |(X_T - X_A)/X_T| \quad X_T \neq 0, \tag{7}$$

where X_T is the true value and X_A is the approximate value.

The measured ^{232}Th, ^{226}Ra and ^{40}K activities of the samples are used to calculate the effective annual dose

Table 3 Dose rate (d*D*/d*t*) and effective annual dose rate (d*E*/d*t*) due to ^{226}Ra, ^{232}Th and ^{40}K in air in granites in Iran

Sample code	Commercial name	Activity (Bq kg^{-1})			d*D*/d*t* (nGy h^{-1})		d*E*/d*t* (mSv year^{-1})	
		^{232}Th	^{226}Ra	^{40}K	Measured[a]	Simulated[b]	Measured	Simulated
G 1	Chayan sable	7.2	4.8	561.4	28.7 ± 1.1	33.7 ± 0.4	0.14	0.17
G 2	Tekab	75.9	39.2	1017.8	101.9 ± 2.4	99.6 ± 0.3	0.50	0.50
G 3	Nehbndan birjand	172.2	99.2	1529.2	204.2 ± 2.9	175.2 ± 0.8	1.00	0.88
G 4	Peranshahr	82.1	53.3	964.7	109.2 ± 1.8	81.6 ± 0.6	0.54	0.41
G 5	Torbat hydaryeh	9.1	10.8	647.5	35.7 ± 1.4	38.1 ± 0.2	0.18	0.19
G 6	Natanz	87.1	58.3	1124.7	120.9 ± 2.6	131.7 ± 0.7	0.59	0.66
G 7	Morvared mashhad	65.6	39.7	941.6	92.9 ± 4.1	47.3 ± 0.5	0.46	0.24
G 8	Akbatan hamedan	65.8	49.6	1144.3	105.1 ± 2.2	71.6 ± 0.3	0.52	0.36
G 9	Sangeh alamot	79.6	43.2	1101.7	109.1 ± 2.1	68.5 ± 0.6	0.54	0.34
G 10	Garmez yazd	59.2	29.9	1047.2	89.4 ± 1.7	96.7 ± 0.4	0.44	0.48
G 11	Balloch zahedan	84.9	41.8	1121.4	112.5 ± 1.6	121.7 ± 0.3	0.55	0.61
G 12	Morvared sabz	73.1	36.8	1002.3	98.7 ± 3.1	70.4 ± 0.5	0.48	0.35
G 13	Khoramdareh	171.3	96.7	1362.7	196.0 ± 5.8	184.4 ± 0.8	0.96	0.92
G 14	Chayan sable	55.9	25.3	811.8	76.1 ± 1.5	86.1 ± 0.4	0.37	0.43
G 15	Tekab	68.1	44.3	1101.4	102.6 ± 2.3	67.6 ± 0.3	0.50	0.34
G 16	Trasheh sfed	148.9	89.3	1341.2	178.7 ± 3.9	160.2 ± 0.6	0.88	0.80
G 17	Morvared sabz	6.5	3.8	556.9	27.7 ± 1.4	26.9 ± 0.2	0.14	0.13
G 18	Hekmtaneh	58.9	39.4	1131.2	96.4 ± 2.6	83.4 ± 0.6	0.47	0.42
G 19	Sangeh lorestan	9.5	5.8	601.8	32.1 ± 1.1	26.3 ± 0.4	0.16	0.13
G 20	Alborz	166.4	79.2	1234.5	180.9 ± 3.6	142.6 ± 0.8	0.89	0.71
Average		77.4	44.5	1017.2	104.9 ± 2.5	90.7	0.51	0.45
Minimum value		6.5	3.8	556.9	27.7	26.3	0.14	0.13
Maximum value		172.2	99.2	1529.2	204.2	184.4	1.00	0.92

[a] Uncertainties are given within 1 standard deviation

[b] Calculation error is under 5%

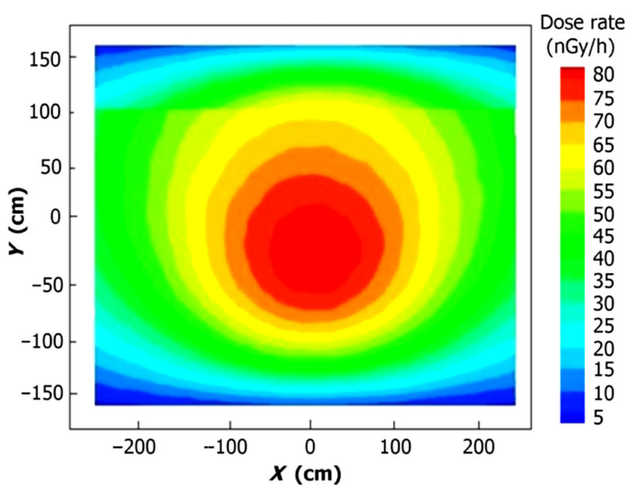

Fig. 1 Absorbed dose rate distribution in the room floor, due to ^{232}Th, ^{226}Ra and ^{40}K

rates, which are 0.14–1.00 mSv year^{-1}, while the simulated effective annual dose rates are 0.13–0.92 mSv year^{-1}.

4 Conclusion

The amount of radiation from natural radionuclides of ^{226}Ra, ^{232}Th and ^{40}K in building materials is determined with a standard room of 5.0 m × 4.0 m × 2.8 m with its floor covered by various granite stones produced in Iran. The dose rates are measured by a gamma-ray spectral system with an HPGe detector and simulated with the MCNP4C code. The two sets of minimum–maximum dose rate range and averaged dose rate show good agreement.

Acknowledgements The authors would like to thank the simulation group in NSTRI of Iran.

References

1. UNSCEAR, United Nations Scientific Committee on the Effects of Atomic Radiation, *Sources and Effects of Ionizing Radiation. Report to the General Assembly with Annexes*, vol. I (United Nations Publications, New York, 2000)
2. S. Kaiser, Radiological protection principles concerning the natural radioactivity of building materials. Radiation Protection 112 (1999)

3. E. Cetin, N. Altinsoy, Y. Örgün, Natural radioactivity levels of granites used in Turkey. Radiat. Prot. Dosim. **151**(2), 299–305 (2012). doi:10.1093/rpd/ncs007
4. A. Faanu, H. Lawluvi, D.O. Kpeglo et al., Assessment of natural and anthropogenic radioactivity levels in soils, rocks and water in the vicinity of Chirano Gold Mine in Ghana. Radiat. Prot. Dosim. **158**(1), 87–99 (2014). doi:10.1093/rpd/nct197
5. S. Dziri, A. Nachab, A. Nourreddine et al., Experimental and simulated effective dose for some building materials in France. World J. Nucl. Sci. Technol. **33**(02), 41 (2013). doi:10.4236/wjnst.2013.32007
6. A. Abbasi, Calculation of gamma radiation dose rate and radon concentration due to granites used as building materials in Iran. Radiat. Prot. Dosim. **155**(3), 335–342 (2013). doi:10.1093/rpd/nct003
7. S. Risica, C. Bolzan, C. Nuccetelli, Radioactivity in building materials: room model analysis and experimental methods. Sci. Total Environ. **272**(1), 119–126 (2001). doi:10.1016/S0048-9697(01)00675-1
8. UNSCEAR, United Nations Scientific Committee on the Effects of Atomic Radiation, *Sources and Effects of Ionizing Radiation, Report to the General Assembly with Annexes*, vol. I (United Nations, NY, 2010)
9. J.F. Briesmeister, MCNPTM-A general Monte Carlo N-particle transport code. Version 4C, LA-13709-M, Los Alamos National Laboratory (2000)
10. Canberra, Genie 2000, Version 3.2. Canberra Industries, Inc, (2005)
11. N.W. El-Dine, A. El-Shershaby, F. Ahmed et al., Measurement of radioactivity and radon exhalation rate in different kinds of marbles and granites. Appl. Radiat. Isot. **55**(6), 853–860 (2001). doi:10.1016/S0969-8043(01)00107-5